Current Climate Change Reports (2019) 5:308–321
https://doi.org/10.1007/s40641-019-00152-9

INTERNAL CLIMATE VARIABILITY (S-P XIE, SECTION EDITOR)

# Indo-Pacific Climate Modes in Warming Climate: Consensus and Uncertainty Across Model Projections

Xiao-Tong Zheng [1,2]

Published online: 25 November 2019


## Abstract

**Purpose of Review** Understanding the changes in climate variability in a warming climate is crucial for reliable projections of future climate change. This article reviews the recent progress in studies of how climate modes in the Indo-Pacific respond to greenhouse warming, including the consensus and uncertainty across climate models.

**Recent Findings** Recent studies revealed a range of robust changes in the properties of climate modes, often associated with the mean state changes in the tropical Indo-Pacific. In particular, the intermodel diversity in the ocean warming pattern is a prominent source of uncertainty in mode changes. The internal variability also plays an important role in projected changes in climate modes.

**Summary** Model biases and intermodel variability remain major challenges for reducing uncertainty in projecting climate mode changes in warming climate. Improved models and research linking simulated present-day climate and future changes are essential for reliable projections of climate mode changes. In addition, large ensembles should be used for each model to reduce the uncertainty from internal variability and isolate the forced response to global warming.

**Keywords** El Niño-Southern Oscillation · Indian Ocean dipole · Indian Ocean basin warming · Indo-western Pacific ocean capacitor · Greenhouse warming · Internal climate variability · Uncertainty in model projections

## Introduction

Internal climate variability in the tropical Indo-Pacific basin significantly impacts the global climate system. Only on interannual timescales, there are several important coupled ocean-atmosphere modes in the region. El Niño-Southern Oscillation (ENSO) is the leading mode of sea-surface temperature (SST) variability in the tropical Pacific. ENSO develops via the coupled positive feedback between the ocean and atmosphere, which is so-called Bjerknes feedback [1, 2]. It influences the global climate through atmospheric and oceanic teleconnections, leading to great environmental and socio-economic impacts [3, 4].

The leading modes of SST variability in the tropical Indian Ocean (TIO) are the Indian Ocean Basin (IOB) and Indian Ocean Dipole (IOD) modes [5]. They also affect regional climate and billions of people in the surrounding regions [6–9]. IOD is an intrinsic mode of Bjerknes feedback [10, 11] in the TIO while the IOB mode is mainly forced by El Niño via atmospheric teleconnections [12, 13]. The maximum basin warming usually occurs in boreal spring, lagging the peak of El Niño by 3–4 months.

Figure 1 shows the evolution of the three modes and their influences on the climate system over the Indo-Pacific region. During boreal summer to autumn, El Niño causes convection to shifts eastward, and the weakened Walker circulation triggers IOD development (Fig. 1a) [14, 15]. During December to February (Fig. 1b), the easterly wind anomalies over the equatorial Indian Ocean (EIO) excite the downwelling Rossby waves in the southern TIO, resulting in the local warming in the southwest IO, where the climatological thermocline is shallow [16]. This southwest IO warming generates an anti-symmetric rainfall/wind pattern across the equator (Fig. 1c) [17], inducing a north Indian Ocean (NIO) warming by

This article is part of the Topical Collection on *Internal Climate Variability*

✉ Xiao-Tong Zheng
zhengxt@ouc.edu.cn

[1] Key Laboratory of Physical Oceanography, Institute for Advanced Ocean Studies, Ocean University of China and Qingdao National Laboratory for Marine Science and Technology, Qingdao 266100, China

[2] Department of Marine Meteorology, College of Oceanic and Atmospheric Sciences, Ocean University of China, Qingdao 266100, China

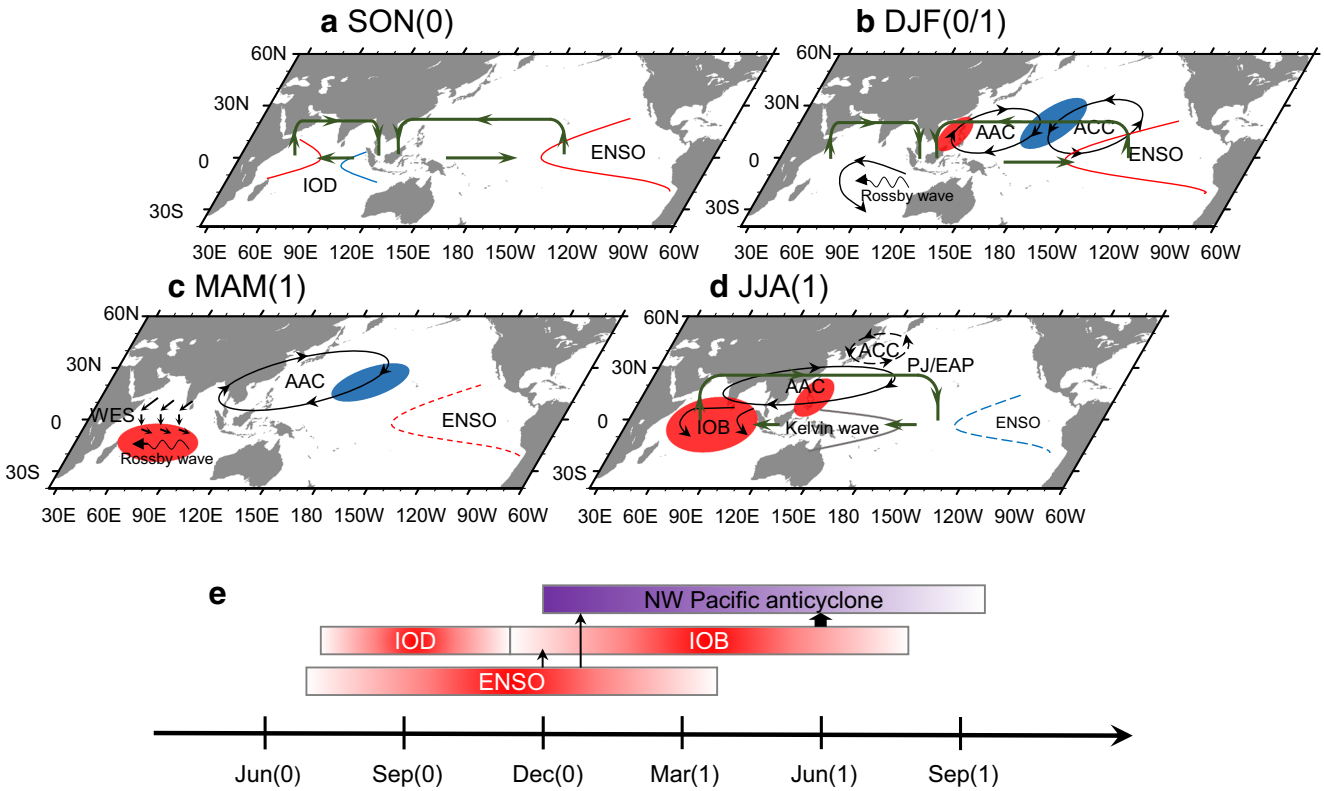


**Fig. 1** **a**–**d** Schematic representation of the major SST anomalies and atmospheric teleconnection over the Indo-Pacific oceans associated with El Niño events (adapted from Fig. 3 in Xie et al. 2016). **a** El Niño develops and interacts with pIOD during September–November; **b** El Niño and pIOD impact on the South IO through westward Rossby waves during December–February; **c** Rossby waves inducing Southwest IO warming, which in turn induces an antisymmetrical wind pattern over the tropical IO during March–May; **d** the second IO warming exciting a tropospheric Kelvin wave propagating into the western Pacific, forcing the AAC and PJ/EAP pattern to affect East Asia during the following summer. **e** Seasonality of major modes of Indo-western Pacific climate variability. Vertical arrows indicate causality, and the block arrow emphasizes the IPOC effect (adapted from Fig. 13 in Xie et al. 2009)

weakening the southwest monsoonal winds (Fig. 1d) [18]. This series of air-sea interactions over the TIO extends the IOB warming through boreal summer following El Niño. In turn, the IOB warming enhances the Walker circulation over the tropical Pacific and leads to a transition from El Niño to La Niña [19].

The interactions between ENSO and IOB are important for the Asia monsoon system (Fig. 1d). When El Niño has matured, a large-scale anomalous low-level anticyclone establishes over the northwest Pacific (NWP) [20–22]. The IOB warming excites a Matsuno-Gill pattern [23, 24], leading to an atmospheric Kelvin wave trough to anchor the northwest Pacific anticyclone (NWPAC) into post-El Niño summer [8, 9, 25]. This NWPAC can affect the East Asia summer monsoon via exciting the Pacific-Japan (PJ) pattern [26], also known as the East Asia-Pacific (EAP) pattern [27]. In addition, the NWPAC interacts with the NIO warming, resulting in positive feedback [28]. Thus, the NWPAC and IOB warming are also an intrinsic mode in the Indo-Pacific, called the Indo-Western Pacific Ocean Capacitor (IPOC) [29].

These coupled modes are the sources of predictability on seasonal to interannual timescales. They exhibit long-term changes in properties, dynamics and climate impacts in observations. For example, ENSO activity in the late twentieth century was anomalously high during the past millennium based on the tree-ring record [30, 31]. The instrumental record also shows the increase in ENSO amplitude after the 1970s [32, 33]. Coincidentally, IOD and IOB both intensified in the twentieth century in paleoclimate and instrumental records [33–35]. These long-term changes in climate modes have not been fully understood. Global warming due to increased greenhouse gases (GHG) is the most significant climate change in the recent century and a half. It is unclear to what degree these ongoing changes are associated with anthropogenic warming. This is one of the most critical questions in current climate research.

Understanding the responses of climate modes to global warming relies on climate model simulations. However, no consensus emerges in the model projections on the amplitude and frequency of these modes [36–39]. In recent years, the response of Indo-Pacific climate modes (ENSO, IOD, and IOB/IPOC) in a warmer climate has been extensively investigated based on state-of-the-art models from the phase 5 of the Coupled Model Intercomparison Project (CMIP5), revealing a series of model consensus. In addition, the sources of

intermodel uncertainty in mode changes were also discussed. This article aims to review the recent progress in the projection of forced changes in tropical Indo-Pacific modes. In the "model consensus" section, we present the robust responses to global warming across models. Most of the robust changes are in the mean state, regulating ocean-atmosphere coupling in the Indo-Pacific region. The "uncertainty" section discusses different sources of intermodel uncertainty in projected changes in climate mode. We show that they are mainly related to the mean state changes. Internal variability also contributes to the uncertainty in mode changes. In the "Summary and Discussions" section, we summarize the progress and discuss ways to reduce uncertainties in projecting climate mode changes. This article focuses on the responses of climate modes to anthropogenic warming. Low-frequency variability of ENSO and other modes during the warm and cold climates in paleoclimate records [40] are beyond the scope of this paper.

## Intermodel Consensus: Mean State Changes in the Tropical Indo-Pacific Oceans

How climate modes change under global warming mainly relies on the ocean-atmosphere mean state changes in the tropical Indo-Pacific [37, 39], which are quite robust across models. Figure 2 shows the mean state responses to global warming associated with climate mode changes. As thermodynamic responses to radiative forcing, the dry static stability in the troposphere increases due to moist adiabatic adjustment (Fig. 2a) [41, 42], while the upper-ocean stratification intensifies because of more heat accumulated in the surface layer (Fig. 2d) [43].

Furthermore, greenhouse warming leads to dynamical mean state responses, such as the spatial pattern of ocean warming and atmospheric circulation change (Fig. 2c). In the tropical Pacific, SST warming peaks on the equator due to reduced evaporative damping [44, 45] and intensifies in the eastern Pacific with a weakened Walker circulation in most models [46]. The easterly wind trend flattens thermocline in the equatorial Pacific (Fig. 2d), maintaining the decrease in zonal SST gradient by suppressing ocean upwelling in the eastern Pacific [47]. This spatial pattern of SST warming, which is quite similar to El Niño on interannual timescales, is called an El Niño-like warming pattern, even though its formation mechanism is different from that of El Niño [37, 45].

Tropical precipitation also shows robust changes in a warmer climate via thermodynamic and dynamic processes [42, 45, 48, 49]. Particularly, ocean surface warming pattern regulates precipitation following the "warmer-gets-wetter" mechanism [45, 50]. It is worth noting that the warming pattern in the tropical Pacific is not consistent among models. Several models even project reduced warming in the eastern equatorial Pacific (i.e., a La Niña-like warming pattern) with an enhanced Walker circulation [51–55].

There are similar dynamical responses of the ocean-atmosphere mean state in the TIO (left in Fig. 2c). The weakened Walker circulation and easterly wind trend lead to less (more) warming and shoaling (deepening) thermocline in the eastern (western) EIO. The spatial pattern of SST change is quite similar to a positive IOD (pIOD) event, called pIOD-like warming pattern [39, 45, 56–58]. The change in precipitation also follows the warmer-gets-wetter mechanism, displaying decrease in the eastern TIO and increase in the western TIO.

The dynamical response of tropical mean state influence climate worldwide under global warming [59]. In particular, through modulating the ocean-atmosphere coupling, the mean state changes affect the properties, dynamics and climate impacts of climate modes in the Indo-Pacific region, such as ENSO, IOD, and IOB.

## ENSO Change Under Greenhouse Warming

How ENSO responds to global warming is one of the most important issues in climate sciences. Numerous studies have been conducted to investigate the response of ENSO to anthropogenic warming by using climate models. However, the complex ocean-atmosphere coupling processes may offset each other, leading to inconsistency in ENSO amplitude or frequency changes among models [37, 60].

Recent studies intensively investigated the response of ENSO to mean state changes, revealing a series of consensus beyond the change in SST amplitude. Firstly, the precipitation of ENSO significantly changes in multimodel projections. Power et al. found that ENSO precipitation variability intensifies and shifts eastward under greenhouse warming in the absence of SST variability change [61]. This robust response is tied to the surface ocean warming pattern in the tropical Pacific, resulting in more extreme precipitation events. Specifically, the enhanced warming in the eastern Pacific reduces the barrier to convective threshold approximated by the tropical mean SST [62], leading to more frequent occurrences of extreme precipitation over the eastern equatorial Pacific during El Niño [63]. This intensification of El Niño-induced precipitation can be reproduced in atmospheric models forced by an El Niño-like warming pattern [61, 64]. Besides, the Maritime continent region warms faster than the central equatorial Pacific, leading to convection easier to move to the Maritime region during La Niña. Therefore, a smaller SST cooling is sufficient to suppress convection over the central Pacific, leading to an increased frequency of extreme La Niña due to the enhanced convective feedback in a warming climate [65]. Recent studies diagnosed ENSO precipitation change in a warming climate by using a decomposition

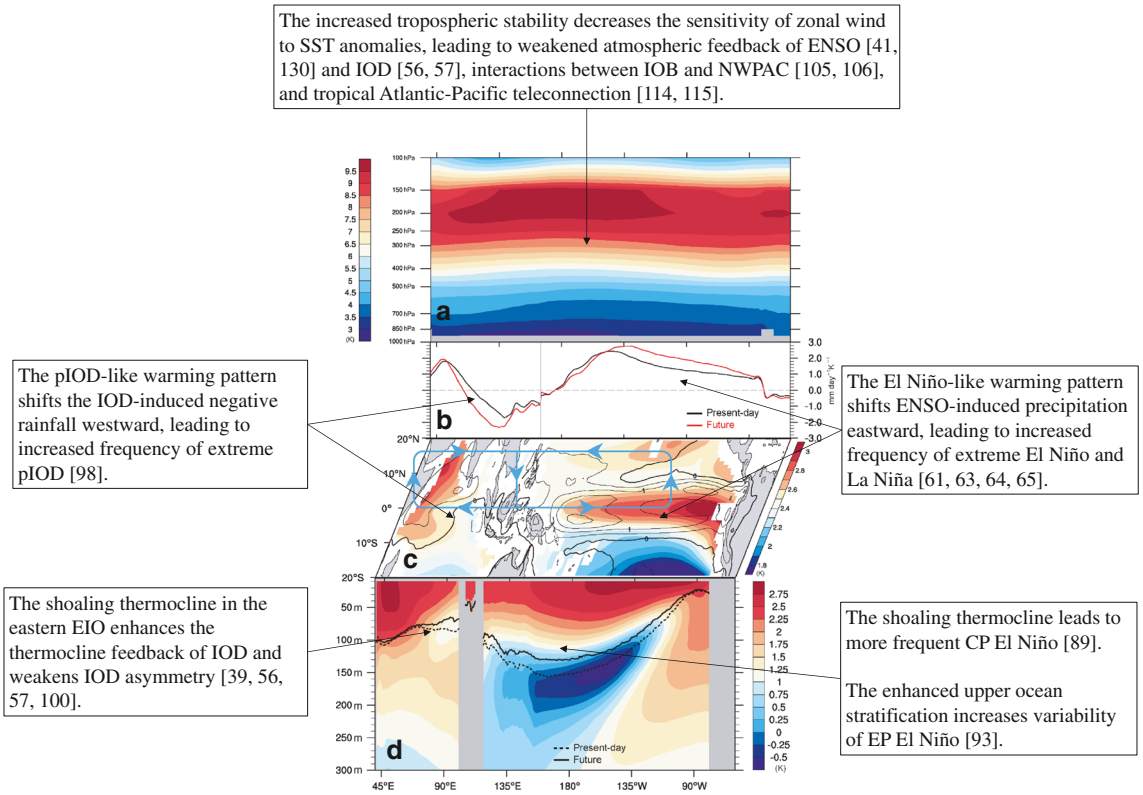


**Fig. 2** The major ocean-atmosphere changes in the Indo-Pacific associated with changes in climate modes. **a** The tropospheric temperature warming along the equator; **b** the present-day (black line) and future (red line) regression of precipitation upon the IOD mode index (left) and ENSO index (right) during September–November and November–January, respectively. **c** The annual mean changes in SST (shading) and precipitation (contour). Blue arrows denote the weakened Walker circulation under global warming. **d** The vertical structure of ocean temperature changes (shading) with thermocline depth (represented by the maximum vertical temperature gradient) in the present-day (dashed line) and future (solid line). All the mean state changes are calculated by the multimodel ensemble mean difference between future climate (2046–2095 in RCP8.5) and present-day climate (1950–1999 in historical simulation) from 34 CMIP5 models. The main effects of mean state changes on climate modes are summarized in the figure

method [66–69]. They found that the mean warming pattern and the structural change in ENSO SST variability both contribute to the changes in ENSO precipitation.

The change in ENSO precipitation further regulates ENSO teleconnections into the extratropics [70, 71]. Specifically, the intensification of ENSO precipitation in the eastern Pacific influences the ENSO-induced Pacific-North America (PNA) pattern [64, 72]. In an atmosphere model forced by an El Niño-like warming pattern in the tropical Pacific, the ENSO-induced PNA pattern intensifies and shifts eastward due to similar changes in ENSO-induced convection anomalies on the equator [64]. Further investigation suggested that the intensification of the PNA teleconnections are more sensitive to the central Pacific (CP) SST anomalies than the eastern Pacific (EP) SST anomalies [73]. Also, the changes in the midlatitude mean flow potentially influence ENSO teleconnections in a warmer climate [74, 75].

It should be noted that owing to the nonlinearity of ENSO, the change in ENSO precipitation is also asymmetric between El Niño and La Niña [76–79]. The El Niño-induced precipitation mostly increases in the eastern equatorial Pacific, while the more suppressed convection appears in the central Pacific during La Niña [63, 65, 80, 81]. The nonlinearity of ENSO SST also changes under greenhouse warming. A weakened asymmetry of ENSO appears in most models due to both oceanic and atmospheric dynamical responses [82, 83].

ENSO diversity or complexity is another essential characteristic of ENSO [84, 85]. Previous studies suggested that there are two types of El Niño in observations and model simulations—the canonical EP El Niño and CP El Niño [86–88]. The increased frequency of CP El Niño in recent decades is regarded as a response to greenhouse warming. Yeh et al. [89] found an increased frequency of the CP El Niño centered at Niño4 region (160° E–150° W, 5° S–5° N) under global warming, compared with that of the EP El Niño centered at Niño3 region (150° W–90° W, 5° S–5° N) in most models. They suggested that the westerly wind trend shoals the thermocline in the western to central equatorial Pacific, increasing local SST variability and leading to more frequent CP El Niño events. However, changes in the intensity and frequency of CP El Niño remains controversial in CMIP5 models [90–92]. Taking into account that the locations of El

Niño differ among models, Cai et al. [93] pointed out that indices of fixed location (e.g., Niño3 and Niño4) cannot well represent the two types of El Niño. Alternatively, they used empirical orthogonal function (EOF) analysis to extract the nonlinearity of ENSO and distinguish the locations of the EP and CP El Niño [94]. Under this definition, the variance of EP El Niño increases under global warming with a robust intermodel consensus. Their further analyses suggested that the enhanced ocean stratification at the zonal wind anomaly center, which locates west of the maximum SST anomaly, is critical for the intensification of EP El Niño via strengthening the ocean-atmosphere coupling [93].

The above consensus is independent of the change in ENSO SST amplitude, which is not consistent among models. However, the SST amplitude of ENSO shows a significant temporal evolution under global warming. Under greenhouse warming, ENSO amplitude increases in the first few decades and then gradually decreases [95]. This non-unidirectional response is related to the change in sensitivity of thermocline to wind forcing in the equatorial Pacific, which is modulated by the unsynchronized warming rate between the tropical Indian Ocean and Pacific.

In addition to dynamical processes, thermodynamical damping also affects ENSO development. Particularly, the cloud-radiation negative feedback is critical for the intensity and frequency of ENSO [96, 97]. The response of ENSO thermodynamics and its contribution to ENSO amplitude change under global warming have not been fully understood.

## Responses of Climate Modes in the TIO to Global Warming

In observations, the occurrence of pIOD gradually increased over the last 150 years [34]. This intensification of IOD is related to the easterly wind trend over the EIO associated with the weakened Walker circulation under global warming (Fig. 2). The easterly wind further shoals the thermocline in the eastern EIO, leading to enhanced thermocline feedback of IOD [39, 56, 57]. However, there is no significant change in IOD amplitude in most models [38, 57]. Further investigations suggested that the increase in atmospheric stability weakens the sensitivity of zonal wind to IOD SST anomalies, offsetting the effect of increased thermocline feedback [56, 57]. The increased occurrence of pIOD in observations is likely to reflect the pIOD-like mean warming pattern. After removing the long-term trend, the pIOD frequency stabilizes both in observations and model projections [39].

Similar to ENSO, the IOD-induced precipitation exhibits a robust response to greenhouse warming. Cai et al. [98] found the anomalous dry condition extending to the central EIO and atmospheric convergence shifting farther west during several strong pIOD years, leading to more extreme climate and weather events. They defined this kind of pIOD event as the extreme pIOD. Under global warming, the pIOD-like warming pattern and easterlies trend over the EIO facilitate the eastern cooling of pIOD strengthening and extending westward (Fig. 2b, c), leading to more extreme pIOD events. Based on the scenario of the Representative Concentration Pathway (RCP) 8.5, the frequency of the extreme pIOD is projected to increase by almost a factor of 3.

The amplitude of pIOD events is usually larger than negative IOD (nIOD) events, which is referred to as the asymmetry of IOD amplitude. The IOD asymmetry is associated with the deep thermocline and nonlinearity of oceanic feedback in the eastern EIO [56, 99, 100]. Shoaling (deepening) thermocline during pIOD (nIOD) causes a stronger (weaker) thermocline-SST feedback, further strengthening (weakening) the amplitude of pIOD (nIOD). In a warming climate, shoaling of the mean thermocline in the eastern EIO decreases the nonlinearity of thermocline-SST feedback, indicating a reduced asymmetry of IOD amplitude in models [47, 100]. The weakening of IOD asymmetry further leads to a positive change of precipitation skewness in the eastern EEIO (not shown). Note that the reduction of IOD asymmetry is not contradictory with the abovementioned increased frequency of extreme pIOD, because the extreme pIOD refers to the dry condition (negative precipitation) over the central EIO [98]. The increased frequency of extreme pIOD characterized by precipitation cannot help increase SST asymmetry in the eastern EIO. The weakened precipitation asymmetry in the eastern EIO and increased extreme precipitation in the CEIO both indicate the westward shift of IOD-induced precipitation anomalies under global warming (Fig. 2b).

For the IOB/IPOC mode, there are some robust changes associated with the local air-sea interaction over the TIO and NWP, despite the mute response of ENSO amplitude. Some studies suggested that the IOB mode will strengthen in a warming climate because of increased water vapor and intensified tropospheric warming over the TIO [101, 102]. The strengthened IOB mode further prolongs the anomalous NWPAC via the IO capacitor effect [101, 103]. In particular, the intensification of anomalous NWPAC is more pronounced following the short decaying El Niño event that fast transits to La Niña, because the NWPAC is further intensified by the enhanced La Niña-induced precipitation anomalies over the central equatorial Pacific [104]. In contrast, some other studies suggested that anomalous NWPAC will weaken in a warmer climate [105, 106]. They pointed out that the increased atmospheric stability weakens Kelvin wave response and reduces the El Niño-related SST gradient between the TIO and the NWP, further attenuates the positive feedback between the NWPAC and IOB warming.

There is also a view that the interaction between the annual cycle and interannual variability plays an essential role in the development of the NWPAC [22, 107, 108]. Thus, the change

in annual cycle under global warming, which shows a seasonal delay of subtropical mean state [109], may also influence the IPOC mode in the future.

## The Role of Interbasin Interactions in Climate Mode Changes

Most of the above studies focused on the effects of local mean state changes (e.g., SST warming pattern, circulation change, stratification change) on the responses of climate modes to global warming. Besides, interbasin interactions over the tropical region is also an important part of internal climate variability and crucial for the development of climate modes [110]. For example, the interactive feedback between ENSO and the TIO climate variability (IOD and IOB) plays a crucial role in the development of these modes [14, 15, 19, 111]. The tropical Atlantic-Pacific teleconnection is also a potential trigger of ENSO [112, 113]. However, the responses of interbasin interactions to greenhouse warming and their potential roles in mode changes have not been fully explored yet. Increased tropospheric stability, which is one of the robust mean state changes, tends to weaken the interbasin interactions. Indeed, the tropical Atlantic-Pacific teleconnection is attenuated in most model projections [114, 115].

There are also interbasin interactions on interdecadal and lower timescales that influence ENSO and other climate modes (see Fig. 3 of Cai et al. [110]). For example, different warming rates between the tropical Pacific and the TIO change the Indo-Pacific zonal SST gradient and thus the mean zonal wind over the equatorial Pacific, further changing ENSO activity via modulating the Bjerknes feedback [95]. The Atlantic decadal variability also affects ENSO intensity and diversity by modulating the mean zonal and meridional winds over the tropical Pacific [116–118]. How these processes change in a warmer climate needs further investigation.

Most abovementioned studies on mode changes are based on high or medium GHG emission scenarios or idealized experiments with a steady increase in radiative forcing to highlight the importance of greenhouse warming. However, the Paris Agreement called for a low-emission scenario to limit global mean temperature (GMT) increase to below 2 °C or even 1.5 °C at the end of the twenty-first century, requiring a "peak-and-decline" GHG emission trajectory. It is also of importance to understand the changes in climate modes under a low-emission scenario. Based on the scenario of RCP2.6 (the lowest emission scenario in CMIP5), Wang et al. [119] reported that the extreme El Niño events would unexpectedly continue to increase after the GMT has stabilized, but not follow the peak-and-decline GHG trajectory. Further investigations suggested that this continued intensification of El Niño precipitation is associated with the slow oceanic response to global warming, which results in similar enhanced warming in the eastern equatorial Pacific after GHG has stabilized [120–122]. These results highlighted the urgency of reducing GHG to avoid more frequent El Niño-related climate extremes in the future. By contrast, the slow SST response in the TIO exhibits a nearly uniform pattern, leading to a stabilized frequency of extreme pIOD after GMT peaks [123].

## Uncertainty: Intermodel Diversity in Changes of Indo-Pacific Climate Modes

Although previous studies obtained a series of consensus on the changes in climate modes, large uncertainties remain across models [37, 39], challenging our understanding of this issue. Some of the abovementioned results are based on a sample of selected models. That is, the related mode changes are more robust in models that well simulate a particular aspect of the climate modes [63, 65, 93, 95, 98]. Recent studies strived to explore the sources of uncertainty in mode changes. Most of them attempted to link the uncertainties with those in mean state changes, which effectively modulate climate modes under global warming.

Among these mean state changes, the SST warming pattern plays a crucial role in modulating climate modes. The intermodel diversity in ENSO amplitude change is closely tied to the spatial pattern of SST warming in the tropical Pacific [124]. In models with enhanced warming in the eastern equatorial Pacific, the mean surface warming reduces the barrier of mean SST to the tropical convection threshold and further intensifies convective feedback and hence interannual SST variability. Since the mean SST warming pattern is a major source of uncertainty in projections for mean precipitation and atmospheric circulation over tropical oceans [125], many other studies suggested that the change in ENSO SST amplitude is also related to those in mean precipitation and atmospheric feedback across models [126–128]. Besides, the mean warming pattern reflects oceanic responses in the tropical Pacific, which potentially influence ENSO amplitude. For example, the change in subtropical cells linked with that of Walker circulation is another potential explanation for the divergent projection of ENSO amplitude change under global warming [129].

Figure 3a shows the scatterplot between the mean warming pattern and ENSO amplitude change among 37 CMIP5 models[1]. Here the Niño3 SST change relative to the tropical mean ($\Delta T^*_{\text{Niño3}}$) represents the spatial pattern of mean warming, and the standard deviation of Niño3 SST ($\sigma T_{\text{Niño3}}$) represents ENSO amplitude. The significant intermodel $\Delta T^*_{\text{Niño3}}$–$\Delta\sigma T_{\text{Niño3}}$ correlation ($r = 0.51$) indicates the importance of the mean warming pattern to ENSO amplitude

[0] Including 34 CMIP5 models with a single run and 3 sets of large ensemble experiments.

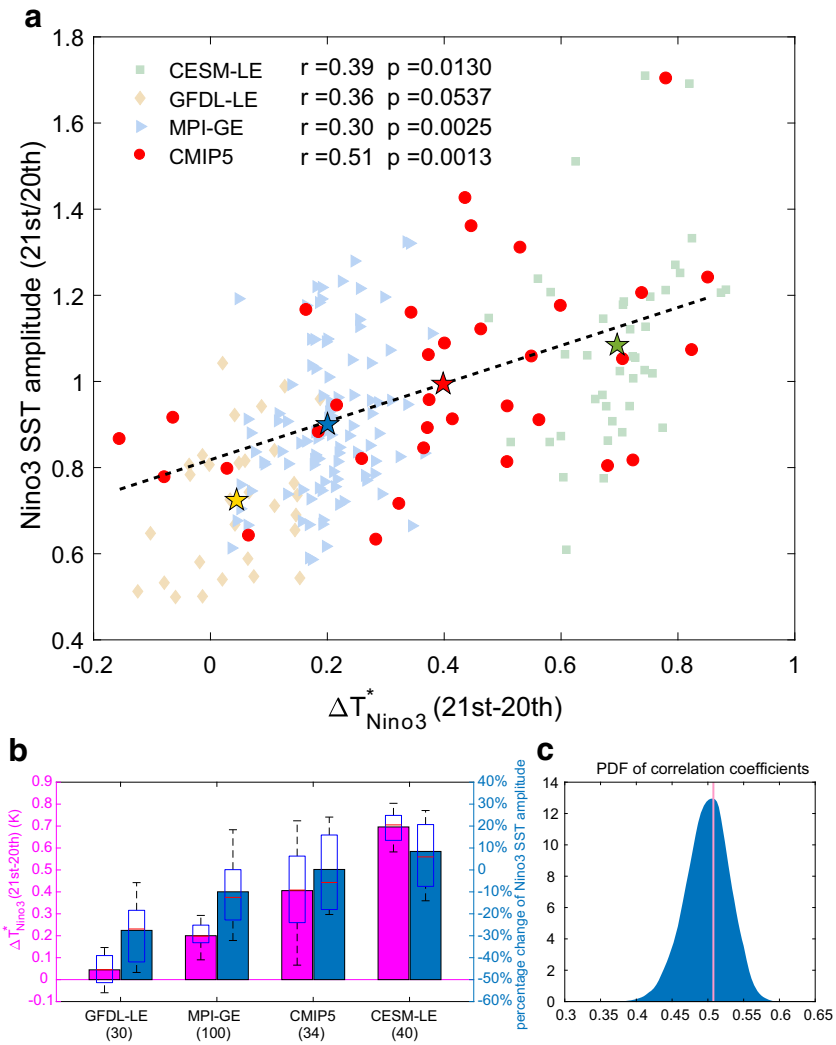


**Fig. 3** **a** Intermodel scatterplots (red dots) between $\Delta T^*_{\text{Niño3}}$ (°C) and the twenty-first- to twentieth-century ratio of standard deviations for Niño3 SST in CMIP5 ensemble. The interember scatterplots from CESM-LE (green square), GFDL-LE (yellow diamond), and MPI-GE (blue triangle) are also shown in (**a**). The red, green, yellow, and blue stars denote the ensemble mean in CMIP5 ensemble, CESM-LE, GFDL-LE, and MPI-GE, respectively. The dashed line denotes the linear regression in CMIP5 ensemble. **b** The multimember ensemble mean $\Delta T^*_{\text{Niño3}}$ (red bar) and percentage change of Niño3 SST amplitude (blue bar) in GFDL-LE, MPI-GE, CMIP5 multimodel ensemble, and CESM-LE. The box-and-whisker plots show the 10th, 25th, 50th, 75th, and 90th percentiles, representing the intermember variability. **c** The percentage histogram of intermodel correlations between $\Delta T^*_{\text{Niño3}}$ and $\sigma T_{\text{Niño3}}$ based on 34 CMIP5 models and three randomly selected members from CESM-LE, GFDL-LE, and MPI-GE. The solid vertical line denotes the intermodel correlation based on 34 CMIP5 models and 3 large ensemble means

change. Similar positive correlations can also be obtained by using the amplitude changes in Niño3 precipitation and Southern Oscillation index instead of Niño3 SST [125]. It should be noted that the horizontal intercept of the $\Delta T^*_{\text{Niño3}}$–$\Delta\sigma T_{\text{Niño3}}$ linear regression is negative, indicating a decreased ENSO amplitude with uniform warming ($\Delta T^*_{\text{Niño3}} = 0$) in tropical oceans. This weakened ENSO activity is associated with decreased atmospheric response to SST anomalies because of the increased tropospheric stability [130].

Intermodel uncertainty in IOD change is also associated with the mean state changes in the TIO. In models with larger shoaling thermocline in the eastern EIO and easterly wind trend along the equator, there are increased amplitude and reduced asymmetry of IOD and vice versa [57, 100]. Although IOD is interactive with ENSO, no intermodel correlation emerges between amplitude changes of the two modes (Fig. 4a) [57]. For the IOB mode, intermodel diversity in amplitude change is significantly correlated with that in ENSO amplitude change (Fig. 4b). By contrast, there is no evidence to show that the intermodel change in IOB amplitude is related to that in local air-sea interactions over the NIO and the NWP [105].

## The Role of Internal Climate Variability

Besides the model uncertainty, internal climate variability is another important source of uncertainty in model projections [131]. Internal variability can regulate not only the warming rate of GMT [132, 133] but also climate modes. In paleoclimatic and instrumental observations, there are significant low-frequency modulations of coupled modes in the Indo-Pacific [30, 31, 35, 134–136]. In models, ENSO amplitude also exhibits pronounced multidecadal modulation interactive with decadal variability in the tropical Pacific. Specifically, a zonal dipole-like tropical Pacific decadal variability is significantly correlated with ENSO amplitude in long-term control run without external forcing [137–141].

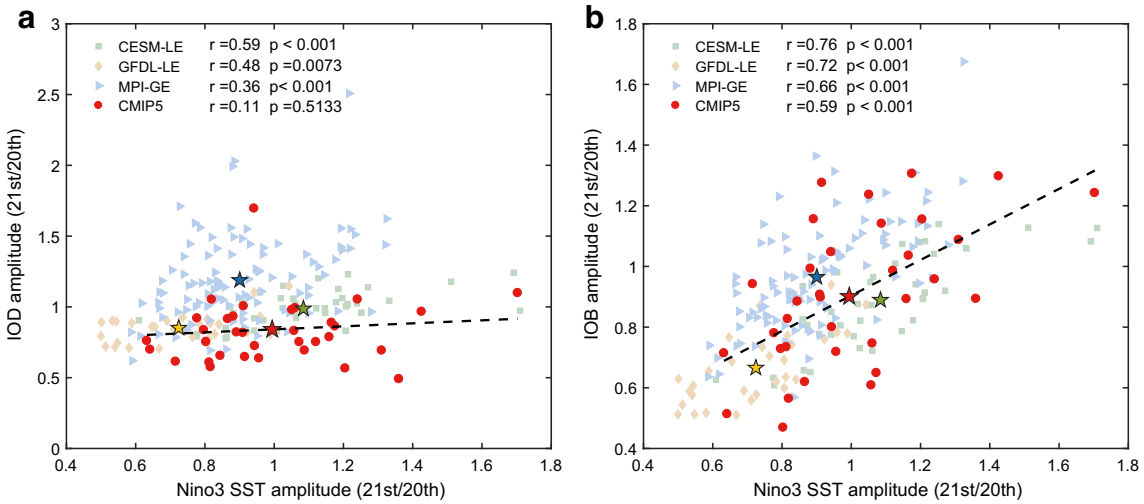


**Fig. 4** Scatterplots of the ratios of Niño3 SST amplitude with **a** IOD amplitude and **b** IOB amplitude between future climate and present-day climate in CMIP5 multimodel ensemble (red dot), CESM-LE (green square), GFDL-LE (yellow diamond), and MPI-GE (blue triangle). The green, yellow, blue, and red stars denote the ensemble mean of CESM-LE, GFDL-LE, MPI-GE, and CMIP5 multimodel, respectively. The dashed line denotes the linear regression in CMIP5 ensemble

Previous studies on projections of climate modes often used a multimodel ensemble (MME) with only one simulation for each model. In this case, the diversity in model projections does not only come from model differences but also partly attributed to internal variability [142, 143]. It is necessary to understand the influence of internal variability on projections of climate modes. Recent studies used large ensemble simulations to assess the effect of internal variability on ENSO future change [144–146]. In a large ensemble experiment, all members use the same model and external forcing with small initialization differences. Thus, the intermember diversity in climate mode changes is solely attributed to internal variability. Based on the large ensemble for Community Earth System Model (CESM-LE) [143], Zheng et al. [144] estimate the influence of internal variability on uncertainty in ENSO projections. The intermember uncertainty in ENSO amplitude change is comparable with the CMIP5 intermodel uncertainty that results from both model response and internal variability. Therefore, it is difficult to disentangle the model response of ENSO from internal variability based on CMIP5 MME with a single ensemble member for each model [146]. A medium ensemble (~ 15 members) is needed to detect the forced response of ENSO amplitude in the CESM RCP8.5 scenario [144].

To assess the influence of internal variability on projected changes in ENSO, we analyzed three sets of large ensemble experiments, which are the 40-member CESM-LE, a 30-member GFDL-ESM2M Large Ensemble (GFDL-LE) [147], and a 100-member MPI-ESM Grand Ensemble (MPI-GE) [148]. All of them are forced by historical and RCP8.5 external forcing until 2100. The spreads in ENSO amplitude change for three large ensembles are all comparable with the CMIP5 intermodel spread (Fig. 3b). By contrast, the intermember uncertainty in $\Delta T^*_{\text{Niño3}}$ for each large ensemble is much lower than that in CMIP5 models, indicating a robust model response of mean warming pattern over the tropics [131, 142]. Also, the relatively large intermodel uncertainty of mean warming indicates that the warming pattern in the tropical Pacific is mainly determined by model biases, such as excessive cold tongue [54, 149], unrealistic cloud-radiation feedback [150] and equatorial ocean dynamics [151].

Comparing the model responses (i.e., the ensemble mean) of three large ensembles and CMIP5 MME mean (bars in Fig. 3b), $\sigma T_{\text{Niño3}}$ tends to increases (decreases) with enhanced (weakened) $\Delta T^*_{\text{Niño3}}$, following the linear $\Delta T^*_{\text{Niño3}}$–$\Delta\sigma T_{\text{Niño3}}$ relationship (Fig. 3a). A similar but weaker $\Delta T^*_{\text{Niño3}}$–$\Delta\sigma T_{\text{Niño3}}$ relationship also exists in each large ensemble. Additionally, internal variability influences the intermodel $\Delta T^*_{\text{Niño3}}$–$\Delta\sigma T_{\text{Niño3}}$ relationship. The intermodel correlation for all models (CMIP5 MME and three large ensembles) varies from 0.35 to 0.6 if only one member is selected to represent each large ensemble (Fig. 3c). Particularly, when the ensemble mean represents the model response for each large ensemble, the intermodel $\Delta T^*_{\text{Niño3}}$–$\Delta\sigma T_{\text{Niño3}}$ correlation is 0.5, near the median of the distribution for all $\Delta T^*_{\text{Niño3}}$–$\Delta\sigma T_{\text{Niño3}}$ correlations.

Internal variability also influences the model projection of IOD change. Hui and Zheng suggested that the intermember uncertainty in IOD amplitude change from CESM-LE is about 40% of that from CMIP5 MME [152]. In large ensembles, the intermember spread in IOD amplitude change is significantly correlated to that in ENSO amplitude change (Fig. 4a), reflecting the importance of ENSO for IOD development. The internal variability of mean thermocline depth in the eastern EIO also influences changes in IOD amplitude and skewness via modulating the Bjerknes positive feedback [153]. The

intermember diversity in IOB amplitude change is highly correlated to that in ENSO amplitude change for all three large ensembles (Fig. 4b). Till now, no study investigates how internal climate variability influences projected changes in local ocean-atmosphere interactions of IOB/IPOC.

## Summary and Discussions

Interannual climate variability has great impacts on global and regional climate. This article reviews the recent progress in the responses of interannual climate modes in the tropical Indo-Pacific to global warming. Based on the state-of-the-art model projections, studies revealed a series of consensus on changes in ENSO, IOD, and IOB/IPOC modes. The spatial pattern of mean ocean warming leads to robust changes in ENSO-related atmospheric anomalies despite the disagreement among models regarding changes in ENSO SST amplitude. Specifically, ENSO precipitation and teleconnections strengthen and shift eastward in most models on account of the enhanced warming in the eastern equatorial Pacific. Mean state changes also influence other properties of ENSO, such as diversity and asymmetry. Similarly, the changes in IOD are associated with the mean state changes in the TIO. For example, the pIOD-like warming pattern leads to an increased frequency of extreme IOD events, while the shoaling thermocline in the eastern EIO weakens the asymmetry of IOD amplitude. For the IOB/IPOC mode, the capacitor effect on anomalous NWPAC weakens, even though the IOB warming seems to strengthen in a warming climate. It is noted that ENSO precipitation will intensify due to slow oceanic warming, leading to a continued increase in extreme El Nino frequency long after the GMT stabilization.

Despite the abovementioned consensus, there are still large intermodel uncertainties in climate mode changes, which are associated with those in mean state changes. Specifically, the spatial pattern of SST warming is a major source of uncertainty in projected ENSO and IOD amplitude change across models. Internal variability is another important source of uncertainty in climate mode changes. The uncertainty in ENSO amplitude change from internal variability is comparable with that from the model response. Reducing the considerable uncertainty in mode changes is in urgent demand for understanding the climate mode changes in a warming climate.

Intermodel uncertainty from the model response is associated with different physics and dynamics across models. Most coupled models still suffer from a lot of common biases such as double ITCZ, excessive cold tongue and overly easterly wind along the EIO [154–156]. These biases influence simulations of the present-day climate modes [36, 157–162] and the mean warming pattern [53, 54, 149, 163, 164], which are both crucial for projected mode changes. Therefore, many abovementioned consensuses on mode changes are based on a sample of selected models with more realistic simulations on the present-day climate (e.g. [63, 65, 93, 95, 98, 105]). Furthermore, previous studies also attempted to link the intermodel diversity of projected ENSO amplitude change with that in the present-day climate simulation [165, 166].

Recently, an emergent constraint (EC) approach is applied to reduce the uncertainty from the model response [167–170]. This approach is based on dynamic mechanisms to find significant relationships between current climate simulations and projected climate changes among models. According to the difference between the present-day climate simulation and observations, we can get the corresponding reliable climate projections. By using the EC approach, previous studies have corrected the mean warming pattern in the tropical Indo-Pacific that is of importance to mode changes [53, 54, 171], implying the feasibility of this approach for correcting the projected climate mode changes. Li et al. [171] used the EC approach to correct the projection of IOD. They suggested that the model biases in the TIO cause a specious pIOD-like warming pattern, further leading to an increased frequency of extreme IOD. After removing the effect of model biases by the EC approach, there is no significant change in the frequency of extreme pIOD. However, given other model biases such as overly shallow eastern EIO thermocline and low eastern EIO SST and rainfall, another study suggested models underestimate the increase in the frequency of extreme pIOD under global warming [172].

Different model biases in the tropical Pacific also have opposite effects on ENSO changes because of complex ENSO dynamics. By using the EC approach to removing the effect of equatorial Pacific cold tongue bias, most models consistently project an El Niño-like warming pattern [53, 54], which favors an increase in ENSO amplitude [125]. In contrast, other studies suggested that a model without the biases of upper-ocean thermal stratification tends to project a La Niña-like warming pattern associated with a weakening of ENSO variability [163, 164]. How to use the EC approach to improve the reliability of climate mode projections still needs further investigation, which requires a better understanding of ocean-atmosphere dynamics in observations and models.

The effect of internal variability on uncertainty in climate projections can be estimated and reduced by large ensembles. However, only a few models provide a large ensemble experiment until now. Here, we suggest large or medium ensembles instead of a single ensemble member for all models to investigate the projected changes in climate modes, despite substantial computational and storage resources required [143]. Based on the multimodel large ensemble, we are able to get the real forced responses of climate modes, which will improve our understanding of intermodel relationships between mean state simulation and climate mode changes. This will further help us reduce uncertainty via the EC approach. Overall, insightful understanding of climate mode dynamics

and improvements in model realism with large simulation samples are essential for reliable projections of climate mode changes in a warming climate.

**Acknowledgments** The author would like to acknowledge useful comments from Dr. Shang-Ping Xie and two anonymous reviewers. The author wishes to thank Dr. Keith Rodgers for sharing the outputs of GFDL-LE. The author also wishes to thank Ms. Chang Hui for preparing the figures in this paper.

**Funding Information** This work was supported by the National Key R&D Program of China (2018YFA0605704), the Natural Science Foundation of China (41975092), and the National Basic Research Program of China (2015CB954300).



## References

1. Bjerknes J. Atmospheric teleconnections from the equatorial Pacific. Mon Wea Rev. 1969;97:163–72.
2. El WK. Niño—the dynamic response of the Equatorial Pacific Ocean to atmospheric forcing. J Phys Oceanogr. 1975;5:572–84.
3. Philander SG. *El Niño, La Niña and the Southern Oscillation*. Academic Press; 1990. p. 293.
4. McPhaden MJ, Zebiak SE, Glantz MH. ENSO as an integrating concept in Earth science. Science. 2006;314:1740–5.
5. Deser C, Alexander MA, Xie S-P, Phillips AS. Sea surface temperature variability: patterns and mechanisms. Annu Rev Mar Sci. 2010;2:115–43.
6. Guan Z, Yamagata T. The unusual summer of 1994 in East Asia: IOD teleconnections. Geophy Res Lett. 2003;30:1544.
7. Ashok K, Guan Z, Saji NH, Yamagata T. Individual and combined influences of ENSO and the Indian Ocean Dipole on the Indian summer monsoon. J Clim. 2004;17:3141–55.
8. Yang J, Liu Q, Xie S-P, Liu Z, Wu L. Impact of the Indian Ocean SST basin mode on the Asian summer monsoon. Geophys Res Lett. 2007;34:L02708.
9. Xie S-P, Hu K, Hafner J, Tokinaga H, Du Y, Huang G, et al. Indian Ocean capacitor effect on Indo-western Pacific climate during the summer following El Niño. J Clim. 2009;22:730–47.
10. Saji NH, Goswami BN, Vinayachandran PN, Yamagata T. A dipole mode in the tropical Indian Ocean. Nature. 1999;401:360–3.
11. Webster PJ, Moore A, Loschnigg J, Leban M. Coupled ocean-atmosphere dynamics in the Indian Ocean during 1997–98. Nature. 1999;401:356–60.
12. Klein SA, Soden BJ, Lau N-C. Remote sea surface temperature variations during ENSO: evidence for a tropical atmospheric bridge. J Clim. 1999;12:917–32.
13. Alexander MA, Bladé I, Newman M, Lanzante JR, Lau N-C, Scott JD. The atmospheric bridge: the influence of ENSO teleconnections on air-sea interaction over the global oceans. J Clim. 2002;15:2205–31.
14. Annamalai H, Xie S-P, McCreary JP, Murtugudde HR. Impact of Indian Ocean sea surface temperature on developing El Niño. J Clim. 2005;18:302–19.
15. Schott FA, Xie S-P, McCreary JP. Indian Ocean circulation and climate variability. Rev Geophys. 2009;47:RG1002.
16. Xie S-P, Annamalai H, Schott FA, McCreary JP. Structure and mechanisms of South Indian Ocean climate variability. J Clim. 2002;15:864–78.
17. Wu RG, Kirtman BP, Krishnamurthy V. An asymmetric mode of tropical Indian Ocean rainfall variability in boreal spring. J Geophys Res. 2008;113(D5):D05104.
18. Du Y, Xie S-P, Huang G, Hu K. Role of air-sea interaction in the long persistence of El Niño-induced north Indian Ocean warming. J Clim. 2009;22:2023–38.
19. Kug J-S, Kang I-S. Interactive feedback between ENSO and the Indian Ocean. J Clim. 2006;19:1784–801.
20. Wang CZ, Weisberg RH, Virmani JI. Western Pacific interannual variability associated with the El Niño-Southern oscillation. J Geophys Res. 1999;104:5131–49.
21. Wang B, Wu RG, Fu XH. Pacific-East Asian teleconnection: how does ENSO affect East Asian climate? J Clim. 2000;13:1517–36.
22. Stuecker MF, Timmermann A, Jin F-F, McGregor S, Ren H-L. A Combination mode of the annual cycle and the El Niño/Southern Oscillation. Nat Geosci. 2013;6:540–4.
23. Matsuno T. Quasi-geostrophic motions in the equatorial area. J Meteor Soc Japan. 1966;44:25–43.
24. Gill AE. Some simple solutions for heat-induced tropical circulation. Quart J Roy Meteor Soc. 1980;106:447–62.
25. Wu B, Li T, Zhou TJ. Relative contributions of the Indian Ocean and local SST anomalies to the maintenance of the western North Pacific anomalous anticyclone during the El Niño decaying summer. J Clim. 2010;23:2974–86.
26. Nitta T. Convective activities in the tropical western Pacific and their impact on the Northern Hemisphere summer circulation. J Meteor Soc Japan. 1987;65:373–90.
27. Huang RH, Sun F. Impact of the tropical western Pacific on the East Asian summer monsoon. J Meteor Soc Japan. 1992;70:213–56.
28. Kosaka Y, Xie S-P, Lau N-C, Vecchi GA. Origin of seasonal predictability for summer climate over the Northwestern Pacific. Proc Natl Acad Sci USA. 2013;110:7574–9.
29. Xie S-P, Kosaka Y, Du Y, Hu K, Chowdary J, Huang G. Indo-western Pacific ocean capacitor and coherent climate anomalies in post-ENSO summer: a review. Adv Atmos Sci. 2016;33:411–32.
30. Li J, Xie S-P, Cook ER, Huang G, D'Arrigo R, Liu F, et al. Interdecadal modulation of El Niño amplitude during the past millennium. Nat Clim Change. 2011;1:114–8.
31. Li J, Xie S-P, Cook ER, Morales M, Christie D, Johnson N, et al. El Niño modulations over the past seven centuries. Nat Clim Change. 2013;3:822–6.
32. An S-I, Wang B. Interdecadal change of the structure of the ENSO mode and its impact on the ENSO frequency. J Clim. 2000;13:2044–55.
33. Xie S-P, Du Y, Huang G, Zheng X-T, Tokinaga H, Hu K, et al. Decadal shift in El Niño influences on Indo-western Pacific and East Asian climate in the 1970s. J Clim. 2010;23:3352–68.
34. Abram NJ, Gagan MK, Cole JE, Hantoro WS, Mudeless M. Recent intensification of tropical climate variability in the Indian Ocean. Nat Geosci. 2008;1:849–53.
35. Chowdary JS, Xie S-P, Tokinaga H, Okumura YM, Kubota H, Johnson NC, et al. Inter-decadal variations in ENSO teleconnection to the Indo-western Pacific for 1870-2007. J Clim. 2012;25:1722–44.
36. Guilyardi E, Wittenberg A, Fedorov A, Collins M, Wang C, Capotondi A, et al. Understanding El Niño in ocean-atmosphere general circulation models: progress and challenges. Bull Amer Meteor Soc. 2009;90:325–40.

37. Collins M, S-I AN, Cai W, Ganachaud A, Guilyardi E, Jin F-F, et al. The impact of global warming on the tropical Pacific Ocean and El Niño. Nat Geosci. 2010;3:391–7.
38. Ihara C, Kushnir Y, Cane MA, de la Peña VH. Climate change over the equatorial Indo-Pacific in global warming. J Clim. 2009;22:2678–93.
39. Cai W, Zheng X-T, Weller E, Collins M, Cowan T, Lengaigne M, et al. Projected response of the Indian Ocean Dipole to greenhouse warming. Nat Geosci. 2013;6:999–1007.
40. Lu Z, Liu Z, Zhu J, Cobb KM. A review of paleo El Niño-Southern Oscillation. Atmosphere. 2018;9:130.
41. Knutson TR, Manabe S. Time-mean response over the tropical Pacific to increased CO2 in a coupled ocean-atmosphere model. J. Clim. 1995;8:2181–99.
42. Held IM, Soden BJ. Robust responses of the hydrological cycle to global warming. J Clim. 2006;19:5686–99.
43. Timmermann A, Oberhuber J, Bacher A, Esch M, Latif M, Roeckner E. Increased El Niño frequency in a climate model forced by future greenhouse warming. Nature. 1999;398:694–7.
44. Liu Z, Vavrus S, He F, Wen N, Zhong Y. Rethinking tropical ocean response to global warming: the enhanced equatorial warming. J Clim. 2005;18:4684–700.
45. Xie S-P, Deser C, Vecchi GA, Ma J, Teng H, Wittenberg AT. Global warming pattern formation: sea surface temperature and rainfall. J Clim. 2010;23:966–86.
46. Vecchi GA, Soden BJ. Global warming and the weakening of the tropical circulation. J Clim. 2007;20:4316–40.
47. Luo Y, Lu J, Liu F, Liu W. Understanding the El Niño-like oceanic response in the tropical Pacific to global warming. Clim Dyn. 2015;45:1945–064.
48. Chou C, Neelin JD. Mechanisms of global warming impact on regional tropical precipitation. J Clim. 2004;17:2688–701.
49. Huang P, Xie S-P, Hu K, Huang G, Huang R. Patterns of the seasonal response of tropical rainfall to global warming. Nat Geosci. 2013;6:357–61.
50. Chadwick R, Boutle I, Martin G. Spatial patterns of precipitation change in CMIP5: why the rich do not get richer in the tropics. J Clim. 2013;26:3803–22.
51. Bayr T, Dommenget D, Martin T, Power SB. The eastward shift of the Walker Circulation in response to global warming and its relationship to ENSO variability. Clim Dyn. 2014;43:2747–63.
52. Lau WKM, Kim K-M. Robust Hadley circulation changes and increasing global dryness due to $CO_2$ warming from CMIP5 model projections. Proc Natl Acad Sci USA. 2015;112:3630–5.
53. Huang P, Ying J. A multimodel ensemble pattern regression method to correct the tropical Pacific SST change patterns under global warming. J Clim. 2015;28:4706–23.
54. Li G, Xie S-P, Du Y, Luo Y. Effect of excessive cold tongue bias on the projections of tropical Pacific climate change. Part I: the warming pattern in CMIP5 multi-model ensemble. Clim Dyn. 2016;47:3817–31.
55. Sohn B-J, Yeh S-W, Lee A, Lau WKM. Regulation of atmospheric circulation controlling the tropical Pacific precipitation change in response to $CO_2$ increases. Nat Commun. 2019;10:1108.
56. Zheng X-T, Xie S-P, Vecchi GA, Liu Q, Hafner J. Indian Ocean dipole response to global warming: analysis of ocean-atmospheric feedbacks in a coupled model. J Clim. 2010;23:1240–53.
57. Zheng X-T, Xie S-P, Du Y, Liu L, Huang G, Liu Q. Indian Ocean Dipole response to global warming in the CMIP5 multimodel ensemble. J Clim. 2013;26:6067–80.
58. Luo Y, Lu J, Liu F, Wan X. The positive Indian Ocean Dipole-like response in the tropical Indian Ocean to global warming. Adv Atmos Sci. 2016;33:476–88.
59. Xie S-P, Deser C, Vecchi GA, Collins M, Delworth TL, Hall A, et al. Towards predictive understanding of regional climate change. Nat Clim Change. 2015;5:921–30.
60. Kim ST, Jin F-F. An ENSO stability analysis. Part II: results from the twentieth and twenty-first century simulations of the CMIP3 models. Clim Dyn. 2011;36:1609–27.
61. Power S, Delage F, Chung C, Kociuba G, Keay K. Robust twenty-first-century projections of El Niño and related precipitation variability. Nature. 2013;502:541–5.
62. Johnson NC, Xie S-P. Changes in the sea surface temperature threshold for tropical convection. Nat Geosci. 2010;3:842–5.
63. Cai W, Borlace S, Lengaigne M, van Rensch P, Collins M, Vecchi G, et al. Increasing frequency of extreme El Niño events due to greenhouse warming. Nat Clim Change. 2014;4:111–6.
64. Zhou Z-Q, Xie S-P, Zheng X-T, Liu Q, Wang H. Global warming-induced changes in El Niño teleconnections over North Pacific and North America. J Clim. 2014;27:9050–64.
65. Cai W, Wang G, Santoso A, McPhaden MJ, Wu L, Jin F-F, et al. Increased frequency of extreme La Niña events under greenhouse warming. Nat Clim Change. 2015;5:132–7.
66. Huang P, Xie S-P. Mechanisms of global warming-induced changes in tropical Pacific rainfall variability associated with ENSO. Nat Geosci. 2015;8:922–6.
67. Bonfils CJ, Santer BD, Phillips TJ, Marvel K, Leung LR, Doutriaux C, et al. Relative contributions of mean-state shifts and ENSO-driven variability to precipitation changes in a warming climate. J Clim. 2015;28:9997–10013.
68. Huang P. Time-varying response of ENSO-induced tropical Pacific rainfall to global warming in CMIP5 models. Part I: multimodel ensemble results. J Clim. 2016;29:5763–78.
69. Huang P. Time-varying response of ENSO-induced tropical Pacific rainfall to global warming in CMIP5 models. Part II: intermodel uncertainty. J Clim. 2017;30:595–608.
70. Perry SJ, McGregor S, Gupta AS, England MH. Future changes to El Niño-Southern Oscillation temperature and precipitation teleconnections. Geophys Res Lett. 2017;44:10608–16.
71. Yeh S-W, Cai W, Min S-K, McPhaden MJ, Dommenget D, Dewitte B, et al. ENSO atmospheric teleconnections and their response to greenhouse gas forcing. Rev Geophys. 2018;56:185–206.
72. Kug J-S, An S-I, Ham Y-G, Kang I-S. Changes in El Niño and La Niña teleconnections over North Pacific-America in the global warming simulations. Theor Appl Climatol. 2010;100:275–82.
73. Chen Z, Gan B, Wu L, Jia F. Pacific-North American teleconnection and North Pacific Oscillation: historical simulation and future projection in CMIP5 models. Clim Dyn. 2018;50:4379–403.
74. Meehl GA, Teng H. Multi-model changes in El Niño teleconnections over North America in a future warmer climate. Clim Dyn. 2007;29:779–90.
75. Schneider EK, Fennessy MJ, Kinter JL III. A statistical-dynamical estimate of winter ENSO teleconnections in a future climate. J Clim. 2009;22:6624–38.
76. Hoerling MP, Kumar A, Zhong M. El Niño, La Niña, and the nonlinearity of their teleconnections. J Clim. 1997;10:1769–86.
77. An S-I, Jin F-F. Nonlinearity and asymmetry of ENSO. J Clim. 2004;17:2399–412.
78. Okumura YM, Deser C. Asymmetry in the duration of El Niño and La Niña. J Clim. 2010;23:5826–43.
79. Zhang T, Sun D. ENSO Asymmetry in CMIP5 models. J Clim. 2014;27:4070–93.
80. Cai W, Santoso A, Wang G, Yeh S-W, An S-I, Cobb KM, et al. ENSO and greenhouse warming. Nat Clim Change. 2015;5:849–59.
81. Huang P, Chen D. Enlarged asymmetry of tropical Pacific rainfall anomalies induced by El Niño and La Niña under global warming. J Clim. 2017;30:1327–43.

82. Ham Y-G. A reduction in the asymmetry of ENSO amplitude due to global warming: the role of atmospheric feedback. Geophys Res Lett. 2017;44:8576–84.
83. Kohyama T, Hartmann DL, Battisti DS. Weakening of nonlinear ENSO under global warming. Geophys Res Lett. 2018;45:8557–67.
84. Capotondi A, Wittenberg AT, Newman M, Di Lorenzo E, Yu J, Braconnot P, et al. Understanding ENSO Diversity. Bull Amer Meteor Soc. 2015;96:921–38.
85. Timmermann A, S-I AN, Kug J-S, Jin F-F, Cai W, Capotondi A, et al. El Niño-Southern Oscillation complexity. Nature. 2018;559:535–45.
86. Kao HY, Yu JY. Contrasting eastern Pacific and central Pacific types of ENSO. J Clim. 2009;22:615–32.
87. Kug J-S, Jin F-F, An S-I. Two types of El Niño events: cold tongue El Niño and warm pool El Niño. J Clim. 2009;22:1499–515.
88. Ashok K, Behera SK, Rao SA, Weng H, Yamagata T. El Niño Modoki and its possible teleconnections. J Geophys Res. 2007;112:C11007.
89. Yeh S-W, Kug J-S, Dewitte B, Kwon M-H, Kirtman B, Jin F-F. El Niño in a changing climate. Nature. 2009;461:511–4.
90. Kim ST, Yu J-Y. The two types of ENSO in CMIP5 models. Geophys Res Lett. 2012;39:L11704.
91. Taschetto AS, Gupta AS, Jourdain NC, et al. Cold tongue and warm pool ENSO events in CMIP5: mean state and future projections. J Clim. 2014;27:2861–85.
92. Xu K, Tam C, Zhu C, Liu B, Wang W. CMIP5 projections of two types of El Niño and their related tropical precipitation in the twenty-first century. J Clim. 2017;30:849–64.
93. Cai W, Wang G, Dewitte B, Wu L, Santoso A, Takahashi K, et al. Increased variability of Eastern Pacific El Niño under greenhouse warming. Nature. 2018;564:201–6.
94. Takahashi K, Montecinos A, Goubanova K, Dewitte B. ENSO regimes: reinterpreting the canonical and Modoki El Niño. Geophys Res Lett. 2011;38:L10704.
95. Kim ST, Cai W, Jin F-F, Santoso A, Wu L, Guilyardi E, et al. Response of El Niño sea surface temperature variability to greenhouse warming. Nat Clim Change. 2014;4:786–90.
96. Rädel G, Mauritsen T, Stevens B, Dommenget D, Matei D, Bellomo K, et al. Amplification of El Niño by cloud longwave coupling to atmospheric circulation. Nat Geosci. 2016;9:106–10.
97. Middlemas EA, Clement AC, Medeiros B, Kirtman B. Cloud radiative feedbacks and El Niño-Southern Oscillation. J Clim. 2019;32:4661–80.
98. Cai W, Santoso A, Wang G, Weller E, Wu L, Ashok K, et al. Increased frequency of extreme Indian Ocean Dipole events due to greenhouse warming. Nature. 2014;51:254–8.
99. Cai W, Qiu Y. An observation-based assessment of nonlinear feedback processes associated with the Indian Ocean Dipole. J Clim. 2013;26:2880–90.
100. Ng B, Cai W, Walsh K. The role of the SST-thermocline relationship in Indian Ocean Dipole skewness and its response to global warming. Sci Rep. 2014;4:6034.
101. Hu K, Huang G, Zheng X-T, Xie S-P, Qu X, Du Y, et al. Interdecadal variations in ENSO influences on Northwest Pacific-East Asian summertime climate simulated in CMIP5 models. J Clim. 2014;27:5982–98.
102. Tao W, Huang G, Hu K, Qu X, Wen G, Gong H. Interdecadal modulation of ENSO teleconnections to the Indian Ocean Basin Mode and their relationship under global warming in CMIP5 models. Int J Climatol. 2015;35:391–407.
103. Zheng X-T, Xie S-P, Liu Q. Response of the Indian Ocean basin mode and its capacitor effect to global warming. J Clim. 2011;24:6146–64.
104. Chen W, Lee J, Ha K, Yun K, Lu R. Intensification of the Western North Pacific anticyclone response to the short decaying El Niño event due to greenhouse warming. J Clim. 2016;29:3607–27.
105. Jiang W, Huang G, Huang P, Hu K. Weakening of Northwest Pacific anticyclone anomalies during post-El Niño summers under global warming. J Clim. 2018;31:3539–55.
106. He C, Zhou T, Li T. Weakened anomalous Western North Pacific anticyclone during an El Niño-decaying summer under a warmer climate: dominant role of the weakened impact of the tropical Indian Ocean on the atmosphere. J Clim. 2019;32:213–30.
107. Stuecker MF, Jin F-F, Timmermann A, McGregor S. Combination mode dynamics of the anomalous Northwest Pacific anticyclone. J Clim. 2015;28:1093–111.
108. Xie S-P, Zhou Z. Seasonal modulations of El Niño-related atmospheric variability: Indo-Western Pacific ocean feedback. J Clim. 2017;30:3461–72.
109. Song F, Leung LR, Lu J, Dong L. Seasonally dependent responses of subtropical highs and tropical rainfall to anthropogenic warming. Nat Clim Change. 2018;8:787–92.
110. Cai W, Wu L, Lengaigne M, Li T, McGregor S, Kug J-S, et al. Pantropical climate interactions. Science. 2019;363:eaav4236.
111. Izumo T, Vialard J, Lengaigne M, Montegut CB, Behera SK, Luo J-J, et al. Influence of the state of the Indian Ocean Dipole on following year's El Niño. Nat Geosci. 2010;3:168–72.
112. Ham Y-G, Kug J-S, Park J-Y, Jin F-F. Sea surface temperature in the north tropical Atlantic as a trigger for El Niño/Southern Oscillation events. Nat Geosci. 2013;6:112–6.
113. Wang L, Yu J-Y, Paek H. Enhanced biennial variability in the Pacific due to Atlantic capacitor effect. Nat Commun. 2017;8:14887.
114. Jia F, Wu L, Gan B, Cai W. Global warming attenuates the tropical Atlantic-Pacific Teleconnection. Sci Rep. 2016;6:20078.
115. Jia F, Cai W, Wu L, Gan B, Wang G, Kucharski F, et al. Weakening Atlantic Niño-Pacific connection under greenhouse warming. Sci Adv. 2019;5:eaax4111.
116. Kang I-S, No H, Kucharski F. ENSO amplitude modulation associated with the mean SST changes in the tropical central Pacific induced by Atlantic multidecadal oscillation. J Clim. 2014;27:7911–20.
117. Li X, Xie S-P, Gille S, Yoo C. Atlantic induced pan-tropical climate change over the past three decades. Nat Clim Change. 2016;6:275–9.
118. Hu S, Fedorov AV. Cross-equatorial winds control El Niño diversity and change. Nat Clim Change. 2018;8:798–802.
119. Wang G, Cai W, Gan B, Wu L, Santoso A, Lin X, et al. Continued increase of extreme El Niño frequency long after 1.5°C warming stabilization. Nat Clim Change. 2017;7:568–72.
120. Held IM, Winton M, Takahashi K, Delworth T, Zeng FR, Vallis GK. Probing the fast and slow components of global warming by returning abruptly to preindustrial forcing. J Clim. 2010;23:2418–27.
121. Long S-M, Xie S-P, Zheng X-T, Liu Q. Fast and slow response to global warming: sea surface temperature and precipitation patterns. J Clim. 2014;27:285–99.
122. Zheng X-T, Hui C, Xie S-P, Cai W, Long S-M. Intensification of El Niño rainfall variability over the tropical Pacific in the slow oceanic response to global warming. Geophys Res Lett. 2019;46:2253–60.
123. Cai W, Wang G, Gan B, Wu L, Santoso A, Lin X, et al. Stabilised frequency of extreme positive Indian Ocean Dipole under 1.5 °C warming. Nat Commun. 2018;9:1419.
124. Zheng X-T, Xie S-P, Lv L-H, Zhou Z-Q. Intermodel uncertainty in ENSO amplitude change tied to Pacific Ocean warming pattern. J Clim. 2016;29:7265–79.

125. Ma J, Xie S-P. Regional patterns of sea surface temperature change: a source of uncertainty in future projections of precipitation and atmospheric circulation. J Clim. 2013;26:2482–501.
126. Watanabe M, Kug J-S, Jin F-F, Collins M, Ohba M, Wittenberg AT. Uncertainty in the ENSO amplitude change from the past to the future. Geophys Res Lett. 2012;39:L20703.
127. An S-I, Choi J. Why the twenty-first century tropical Pacific trend pattern cannot significantly influence ENSO amplitude? Clim Dyn. 2015;44:133–46.
128. Rashid HA, Hirst AC, Marsland SJ. An atmospheric mechanism for ENSO amplitude changes under an abrupt quadrupling of CO2 concentration in CMIP5 models. Geophys Res Lett. 2016;43:1687–94.
129. Chen L, Li T, Yu Y, Behera SK. A possible explanation for the divergent projection of ENSO amplitude change under global warming. Clim Dyn. 2017;49:3799–811.
130. Huang P, Chen D, Ying J. Weakening of the tropical atmospheric circulation response to local sea surface temperature anomalies under global warming. J Clim. 2017;30:8149–58.
131. Hawkins E, Sutton R. The potential to narrow uncertainty in regional climate predictions. Bull Am Meteor Soc. 2009;90:1095–107.
132. Kosaka Y, Xie S-P. Recent global-warming hiatus tied to equatorial Pacific surface cooling. Nature. 2013;501:403–7.
133. Kosaka Y. Xie S-P The tropical Pacific as a key pacemaker of the variable rates of global warming. Nat Geosci. 2016;9:669–73.
134. Ashok K, Chan W-L, Motoi T, Yamagata T. Decadal variability of the Indian Ocean Dipole. Geophys Res Lett. 2004;31:L24207.
135. Sadekov AY, Ganeshram R, Pichevin L, Berdin R, McClymont E, Elderfield H, et al. Palaeoclimate reconstructions reveal a strong link between El Niño-Southern Oscillation and Tropical Pacific mean state. Nat Commun. 2013;4:2692.
136. Han W, Vialard J, McPhaden MJ, Lee T, Masumoto Y, Feng M, et al. Indian Ocean decadal variability: a review. Bull Amer Meteor Soc. 2014;95:1679–703.
137. Rodgers KB, Friederichs P, Latif M. Tropical Pacific decadal variability and its relation to decadal modulations of ENSO. J Clim. 2004;17:3761–74.
138. Yeh S-W, Kirtman B. Tropical Pacific decadal variability and ENSO amplitude modulation in a CGCM. J Geophys Res. 2004;109:C11009.
139. Wittenberg AT. Are historical records sufficient to constrain ENSO simulations? Geophys Res Lett. 2009;36:L12702.
140. Ogata T, Xie S-P, Wittenberg AT, Sun D-Z. Interdecadal amplitude modulation of El Niño/Southern Oscillation and its impacts on tropical Pacific decadal variability. J Clim. 2013;26:7280–97.
141. Stevenson SL. Significant changes to ENSO strength and impacts in the twenty-first century: Results from CMIP5. Geophy Res Lett. 2012;39:L17703.
142. Deser C, Knutti R, Solomon S, Phillips AS. Communication of the role of natural variability in future North American climate. Nat Clim Change. 2012;2:775–9.
143. Kay JE, Deser C, Phillips A, Mai A, Hannay C, Strand G, et al. The community earth system model (CESM) large ensemble project: a community resource for studying climate change in the presence of internal climate variability. Bull Am Meteorol Soc. 2015;96:1333–49.
144. Zheng X-T, Hui C, Yeh S-W. Response of ENSO amplitude to global warming in CESM large ensemble: uncertainty due to internal variability. Clim Dyn. 2018;50:4019–35.
145. Vega-Westhoff B, Sriver RL. Analysis of ENSO's response to unforced variability and anthropogenic forcing using CESM. Sci Rep. 2017;7:18047.
146. Maher N, Matei D, Milinski S, Marotzke J. ENSO change in climate projections: forced response or internal variability? Geophys Res Lett. 2018;45:11390–8.
147. Rodgers KB, Lin J, Frölicher TL. Emergence of multiple ocean ecosystem drivers in a large ensemble suite with an Earth system model. Biogeosciences. 2015;12:3301–20.
148. Maher N, Milinski S, Suarez-Gutierrez L, Botzet M, Dobrynin M, Kornblueh L, et al. The Max Planck Institute Grand Ensemble: enabling the exploration of climate system variability. J Adv Model Earth Sy. 2019;11:1–21.
149. Ying J, Huang P, Lian T, Tan H. Understanding the effect of an excessive cold tongue bias on projecting the tropical Pacific SST warming pattern in CMIP5 models. Clim Dyn. 2019;52:1805–18.
150. Ying J, Huang P. Cloud-radiation feedback as a leading source of uncertainty in the tropical Pacific SST warming pattern in CMIP5 models. J Clim. 2016;29:3867–81.
151. Ying J, Huang P. The large-scale ocean dynamical effect on uncertainty in the tropical Pacific SST warming pattern in CMIP5 models. J Clim. 2016;29:8051–65.
152. Hui C, Zheng X-T. Uncertainty in Indian Ocean Dipole response to global warming: the role of internal variability. Clim Dyn. 2018;51:3597–611.
153. Ng B, Cai W, Cowan T, Bi D. Influence of internal climate variability on Indian Ocean Dipole properties. Sci Rep. 2018;8:13500.
154. Li G, Xie S-P. Tropical biases in CMIP5 multi-model ensemble: the excessive equatorial Pacific cold tongue and double ITCZ problems. J Clim. 2014;27:1765–80.
155. Li G, Xie S-P, Du Y. Monsoon-induced biases of climate models over the tropical Indian Ocean with implications for regional climate projection. J Clim. 2015;28:3058–72.
156. Li G, Xie S-P, Du Y. Climate model errors over the South Indian Ocean thermocline dome and their effect on the basin mode of interannual variability. J. Clim. 2015;28:3093–8.
157. Bellenger H, Guilyardi E, Leloup J, Lengaigne M, Vialard J. ENSO representation in climate models: from CMIP3 to CMIP5. Clim Dyn. 2013;42:1999–2018.
158. Ham Y-G, Kug J-S. Improvement of ENSO simulation based on Intermodel diversity. J Clim. 2015;28:998–1015.
159. Cai W, Cowan T. Why is the amplitude of the Indian Ocean Dipole overly large in CMIP3 and CMIP5 climate models? Geophys Res Lett. 2013;40:1200–5.
160. Du Y, Xie S-P, Yang Y-L, Zheng X-T, Liu L, Huang G. Indian Ocean variability in the CMIP5 multi-model ensemble: the basin mode. J Clim. 2013;26:7240–66.
161. Liu L, Xie S-P, Zheng X-T, Li T, Du Y, Huang G, et al. Indian Ocean variability in the CMIP5 multi-model ensemble: the zonal dipole mode. Clim Dyn. 2014;43:1715–30.
162. Zheng X-T, Gao L, Li G, Du Y. The southwest Indian Ocean thermocline dome in CMIP5 models: historical simulation and future projection. Adv Atmos Sci. 2016;33:489–503.
163. Kohyama T, Hartmann DL, Battisti DS. La Niña-like mean-state response to global warming and potential oceanic roles. J Clim. 2017;30:4207–25.
164. Kohyama T, Hartmann DL. Nonlinear ENSO warming suppression (NEWS). J Clim. 2017;30:4227–51.
165. Ham Y-G, Kug J-S. ENSO amplitude changes due to greenhouse warming in CMIP5: role of mean tropical precipitation in the twentieth century. Geophys Res Lett. 2016;43:422–30.
166. Ying J, Huang P, Lian T, Chen D. Intermodel uncertainty in the change of ENSO's amplitude under global warming: role of the response of atmospheric circulation to SST anomalies. J Clim. 2019;32:369–83.
167. Boe JL, Hall A, Qu X. September sea-ice cover in the Arctic Ocean projected to vanish by 2100. Nat Geosci. 2009;2:341–3.
168. Cox PM, Pearson D, Booth BB, Friedlingstein P, Huntingford C, Jones CD, et al. Sensitivity of tropical carbon to climate change constrained by carbon dioxide variability. Nature. 2013;494:341–4.

169. Li G, Xie S-P, He C, Chen Z. Western Pacific emergent constraint lowers projected increase in Indian summer monsoon rainfall. Nat Clim Change. 2017;7:708–12.
170. Hall A, Cox P, Huntingford C, Klein S. Progressing emergent constraints on future climate change. Nat Clim Change. 2019;9:269–78.
171. Li G, Xie S-P, Du Y. A robust but spurious pattern of climate change in model projections over the tropical Indian Ocean. J Clim. 2016;29:5589–608.
172. Wang G, Cai W, Santoso A. Assessing the impact of model biases on the projected increase in frequency of extreme positive Indian Ocean Dipole events. J Clim. 2017;30:2757–67.